In: Financial Markets
Editors: M. Bahmani-Oskooee and S. Bahmani
ISBN: 978-1-62948-420-4

Chapter 6

WITH STRINGS TOWARD SAFETY FUTURE ON FINANCIAL MARKETS

Richard Pincak*
Institute of Experimental Physics, Slovak Academy of Sciences,
Watsonova, Kosice, Slovak Republic
Bogoliubov Laboratory of Theoretical Physics,
Joint Institute for Nuclear Research, Dubna, Moscow Region, Russia

Abstract

Almost all known econometric models applied on a long term basis on financial forex market do not work sufficiently. The reason is that transaction costs and arbitrage opportunity are not included, as this does not simulate the real financial markets. Analyzes are not done on the non equidistance date but rather on the aggregate date, which is also not a real financial case. Almost all known prediction models are not stable for longer in treading on the financial forex market. In this chapter we would like to show a new way how to analyze and, moreover, forecast financial market. We utilize the projections of the real exchange rate dynamics onto the string-like topology. Our approach is inspired by the contemporary movements in the string theory. Inter-strings information transfer is analyzed as an analogy with dynamic of prices or currency at specified exchange rate options.

PACS 11.25.Wx, 89.65.Gh, 89.90.+n

Keywords: quantitative finance, string theory, trading strategy, financial forecasting, risk management

1. Introduction

We are currently in the process of transfer of modern physical ideas into the neighboring field called econophysics. The physical statistical view point has proved fruitful, namely, in the description of systems where many-body effects dominate. However, standard, accepted by physicists, bottom-up approaches are cumbersome or outright impossible to follow the

*E-mail address: pincak@saske.sk

behavior of the complex economic systems, where autonomous models encounter the intrinsic variability. We would like to transfer modern physics ideas into neighboring field called econophysics.

Digital economy is founded on data. In the chapter, we suggest and analyze statistical properties of heuristics based on the currency rate data which are arranged to mimic the topology of the basic variants of the physical strings and branes. Our primary motivation comes from the actual physical concepts [1, 2]; however, our realization differs from the original attempts in various significant details. The second aspect of our method is that it enables a transformation into a format which is useful for an analysis of a partial trend or relative fluctuations on the time scale window of interest.

As with most science problems, the representation of data is the key to efficient and effective solutions. The underlying link between our approach and the string theory may be seen in the switching from a local to a non-local form of the data description. This line passes from the single price to the multivalued collection of prices from the temporal neighborhood which we term here the string map. As we will see later, an important role in our considerations is played by the distance measure of the string maps. The idea of exploring the relationship between more intuitive geometric methods and financial data is not new. The discipline called the geometric data analysis includes many diverse examples of the conceptual schemes and theories grounded on the geometric representation and properties of data. Among them we can emphasize the tree network topology that exhibits usefulness in the studies of the world-trade network [3] and other network structures of the market constructed by means of inter-asset correlations [4, 5]. The multivariate statistical method called *cluster analysis* deals with data mapping onto representative subsets called *clusters* [6]. Here we work on the concept that is based on projection data into higher dimensional vectors in the sense of the work [7, 8]. Also, arguments based on the metrics are consistent with our efforts but not too obvious points in common with the original objectives of the nonlinear analysis.

The string theory development over the past 25 years achieved a high degree of popularity among physicists [9, 10]. The reason lies in its inherent ability to unify theories that come from diverse physical spheres. The prime instrument of the unification represents the concept of extra dimension. The side-product of theoretical efforts can be seen in the elimination of the ultraviolet divergences of Feynman diagrams. However, despite the considerable achievements, there is a lack of the experimental verification of the original string theory. In contrast, in the present work we exploit time-series which can build the family of the string motivated models of boundary-respecting maps. In a narrow sense, the purpose of the present data-driven study is to develop statistical techniques for the analysis of these objects.

Time series forecasting is a scientific field under continuous active development covering an extensive range of methods. Traditionally, linear methods and models are used. Despite their simplicity, linear methods often work well and may well provide an adequate approximation for the task at hand and are mathematically and practically convenient. However, the real life generating processes are often non-linear. This is particularly true for financial time series forecasting. Therefore the use of non-linear models is promising. Many observed financial time series exhibit features which cannot be explained by a linear model. We derive two models for predictions of EUR/USD prices on the forex market. This is the first attempt for real application of the string theory in the field of finance, and not only in high energy physics, where it is established very well.

There are plenty of non-linear forecast models based on different approaches (e.g. GARCH [11], ARCH [12], ARMA [13], ARIMA [14] etc) used in financial time series forecasting. Currently, perhaps the most frequently used methods are based on Artificial Neural Networks (ANN, which covers a wide range of methods) and Support Vector Machines (SVM). A number of research articles compare ANN and SVM to each other and to other more traditional non-linear statistical methods. Tay and Cao ([15]) examined the feasibility of SVM in financial time series forecasting and compared it to a multilayer Back Propagation Neural Network (BPNN). They showed that SVM outperforms the BP neural network. Kamruzzaman and Sarker [16] modeled and predicted currency exchange rates using three ANN based models and a comparison was made with the ARIMA model. The results showed that all the ANN based models outperform the ARIMA model. Chen et al. [17] compared SVM and BPNN taking the auto-regressive model as a benchmark in forecasting the six major Asian stock markets. Again, both the SVM and BPNN outperformed the traditional models.

While the traditional ANN implements the empirical risk minimization principle, SVM implements the structural risk minimization ([18]). Structural risk minimization is an inductive principle for model selection used for learning from finite training data sets. It describes a general model of capacity control and provides a trade-off between hypothesis space complexity and the quality of fitting the training data (empirical error). For this reason SVM is often chosen as a benchmark to compare other non-linear models to. Also, there is a growing number of novel and hybrid approaches, combining the advantages of various methods using for example evolutionary optimization, methods of computational geometry and other techniques (e.g. [19], [20]).

In the present chapter we also exploits time series which can build the family of the string-motivated models of boundary-respecting maps. The purpose of the present data-driven study is to develop statistical techniques for the analysis of these objects and moreover for the utilization of such string models onto the forex market. Both of the string prediction models in this paper are built on the physical principle of the invariance in time series of the forex market. Founding of a stationary state in the time series of the market was studied in [21]

2. Data Analysis

First of all we need to mention some facts about data streams we analyzed. We analyze tick by tick data of EUR/USD, GBP/USD, USD/JPY, USD/CAD, USD/CHF major currency pairs from the OANDA market maker. We focussed on the three month period within three selected periods of 2009 which capture moments of the financial crisis. The streams are collected in such a way that each stream begins with Monday. More precisely, we selected periods denoted as Aug-Sep (from August 3rd. to September 7th.), Sep-Oct (Sep.7-Oct.5) and Oct-Nov (Sep.5-Nov.2). At first, the data sample has been decimated - only each 10th tick was considered. This delimits results to the scales larger than 10 ticks. The mean time corresponding to the string length l_s in ticks is given by

$$T(l_s) = \langle t(\tau + l_s) - t(\tau) \rangle \simeq \frac{1}{\tau_{up} - \tau_{dn}} \sum_{\tau=\tau_{dn}}^{\tau_{up}} [t(\tau + l_s) - t(\tau)] \,. \qquad (1)$$

3. One Dimensional Maps

By applying standard methodologies of detrending one may suggest to convert original series of the quotations of the mean currency exchange rate $p(\tau)$ onto a series of returns defined by

$$\frac{p(\tau + h) - p(\tau)}{p(\tau + h)} \,, \qquad (2)$$

where h denotes a tick lag between currency quotes $p(\tau)$ and $p(\tau + h)$, τ is the index of the quote. The mean $p(\tau) = (p_{ask}(\tau) + p_{bid}(\tau))/2$ is calculated from $p_{ask}(\tau)$ and $p_{bid}(\tau)$.

In the spirit of the string theory it would be better to start with the 1-end-point open string map

$$P^{(1)}(\tau, h) = \frac{p(\tau + h) - p(\tau)}{p(\tau + h)} \,, \qquad h \in < 0, l_s > \qquad (3)$$

where superscript (1) refers to the number of endpoints.

Later, we may use the notation $P\{p\}$ which emphasizes the functional dependence upon the currency exchange rate $\{p\}$. It should also be noted that the use of P highlights the canonical formal correspondence between the *rate of return* and the internal *string momentum*.

Here the tick variable h may be interpreted as a variable which extends along the extra dimension limited by the string size l_s. A natural consequence of the transform, Eq.(3), is the fulfilment of the boundary condition

$$P^{(1)}(\tau, 0) = 0 \,, \qquad (4)$$

which holds for any tick coordinate τ. Later on, we want to highlight effects of the rare events. For this purpose, we introduce a power-law q-deformed model

$$P_q^{(1)}(\tau, h) = f_q \left(\frac{p(\tau + h) - p(\tau)}{p(\tau + h)} \right) \,, \qquad h \in < 0, l_s > \qquad (5)$$

by means of the function

$$f_q(x) = \text{sign}(x) \, |x|^q \,, \qquad q > 0 \,. \qquad (6)$$

The 1-end-point string has defined the origin, but it reflects the linear trend in $p(.)$ at the scale l_s. Therefore, the 1-end-point string map $P_q^{(1)}(.)$ may be understood as a q-deformed generalization of the *currency returns*. The illustration of the 1-end-point model is given in Fig.(1). The corresponding statistical characteristics displayed in Fig.(2) have been obtained on the basis of a statistical analysis discussed in section 2..

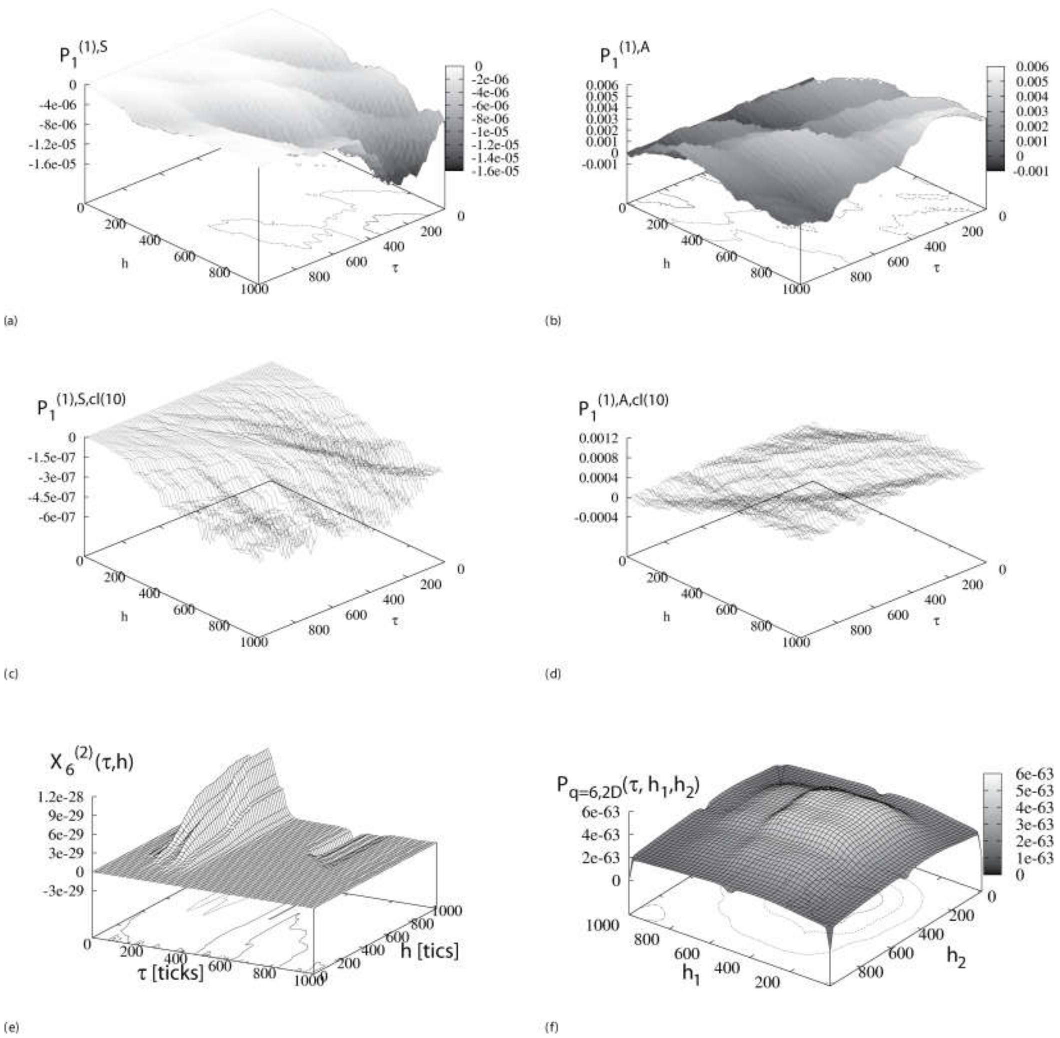

Figure 1. The illustrative examples of the currency data map for GBP/USD. The parts (a)-(d) constructed for date Fri, 31 Jul 2009 time interval 15:06:37 - 15:43:09 GMT. Time evolution of symmetric ($P^{(1),\mathrm{S}}_{q=1}$) and anti-symmetric ($P^{(1),\mathrm{A}}$) component of the 1-end-point string of size $l_{\mathrm{s}} = 1000$ calculated for $q = 1$ (by means of Eq.(23)). In (c),(d) we see the same data mapped by means of the partially closed 1-end-point string ($q = 1$) for $N_{\mathrm{m}} = 10$, according to Eq.(31)). (e) The calculation carried out for the 2-end-point string for $l_{\mathrm{s}} = 1000$, $q = 6$ at some instant. We see that conjugate variable $X^{(2)}_{q=6}(\tau, h)$ satisfies the Neumann-type boundary conditions; (f) The instantaneous 2D-Brane state (date Fri, 31 Jul 2009 15:11:47 GMT) is computed according to Eq.(28).

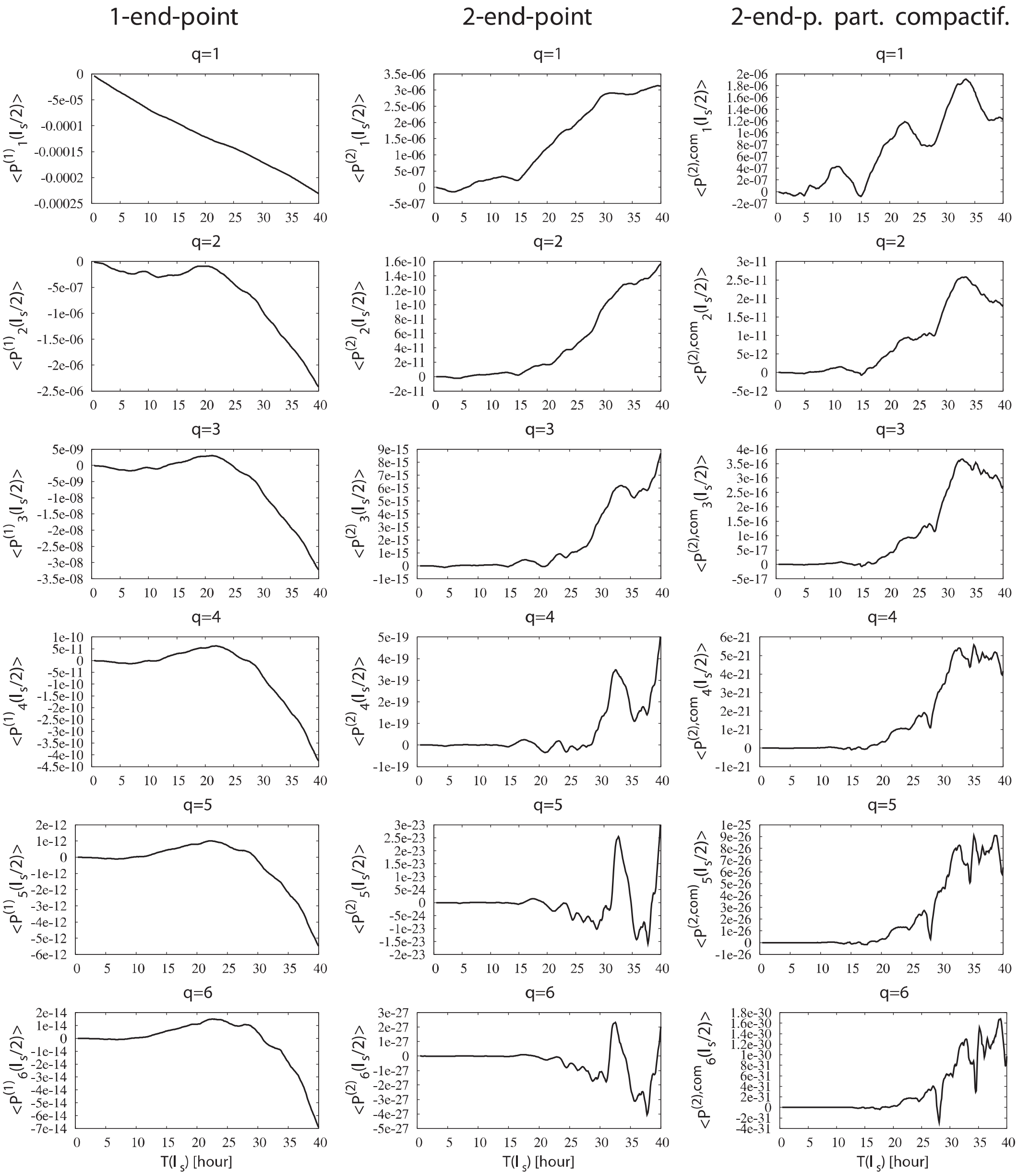

Figure 2. The variability in statistical characteristics caused by differences in topology and q. Calculated for the period Aug-Sep, GBP/USD currency. The model with $q = 1$ has ability to reveal the currency long trend, on the other hand, the rare events are better visible for the 2-end-point string. The effect of the partial compactification with $N_{\rm m} = 4$ [see Eq.(31)] is demonstrated in the third column (again for the 2-end-point string).

Clearly, the situation with a long-term trend is partially corrected by fixing $P_q^{(2)}(\tau, h)$ at $h = l_{\rm s}$. The open string with two end points is introduced via the nonlinear map which combines information about trends of p at two sequential segments

$$P_q^{(2)}(\tau, h) = f_q\left(\left(\frac{p(\tau+h)-p(\tau)}{p(\tau+h)}\right)\left(\frac{p(\tau+l_{\rm s})-p(\tau+h)}{p(\tau+l_{\rm s})}\right)\right), \qquad h \in < 0, l_{\rm s} > \ . \tag{7}$$

The map is suggested to include boundary conditions of *Dirichlet type*

$$P_q^{(2)}(\tau, 0) = P_q(\tau, l_{\rm s}) = 0\,, \qquad \text{at all ticks } \ \tau\,. \tag{8}$$

In particular, the sign of $P_q^{(2)}(\tau, h)$ comprises information about the behavior differences of $p(.)$ at three quotes $(\tau,\ \tau+h,\ \tau+l_{\rm s})$. The $P_q^{(2)}(\tau, h) < 0$ occurs for trends of the different sign, whereas $P_q^{(2)}(\tau, h) > 0$ indicates the match of the signs.

In addition to the variable $P_q^{(2)}(\tau, h)$ we introduced the conjugate variable $X_q^{(2)}(\tau)$ via the recurrent summation

$$X_q^{(2)}(\tau, h+1) = X_q^{(2)}(\tau, h) + P_q^{(2)}(\tau, h-1)\,[\,t(\tau+h) - t(\tau+h-1)\,] \tag{9}$$

(here $t(.)$ stands for a time-stamp corresponding to the quotation index τ in the argument). The above discrete form is suggested on the basis of the time-continuous Newton second law of motion $\dot{X}_q^{(2)}(t, h) = P_q^{(2)}(t, h)$ (written here for a unit mass). The form is equivalent to the imposing of the quadratic kinetic energy term $\frac{1}{2}(P_q^{(2)})^2$. Thus, the Hamiltonian picture [10] can be reconstructed in the following way;

$$\mathcal{H} = \frac{1}{2}\sum_{h=0}^{l_{\rm s}}\left[(\,P_q^{(2)}(\tau, h)\,)^2 - [\phi_{\rm ext}(\tau, h+1) - \phi_{\rm ext}(\tau, h)]\ X_q^{(2)}(\tau, h)\right], \tag{10}$$

where $\phi_{\rm ext}(\tau, h)$ is the external field term which depends on the transform of the currency rate [see e.g. Eq.(7)]. We pass from the continuum to discrete theory by means of the functional form

$$\dot{P}_q^{(2)} \;=\; -\frac{\delta\mathcal{H}}{\delta X_q^{(2)}(h)} = \phi_{\rm ext}(\tau, h+1) - \phi_{\rm ext}(\tau, h) = P_q^{(2)}(\tau, h+1) - P_q^{(2)}(\tau, h)\,, \tag{11}$$

where $P_q^{(2)}(\tau, h)$ can be calibrated equal to $\phi_{\rm ext}(\tau, h)$.

The discrete conjugate variable meets the *Neumann type* boundary conditions

$$X_q^{(2)}(\tau, 0) = X_q^{(2)}(\tau, 1)\,, \qquad X_q^{(2)}(\tau, l_{\rm s}-1) = X_q^{(2)}(\tau, l_{\rm s})\,, \tag{12}$$

which is illustrated in Fig.(1)(d).

A more systematic way to obtain the 2-end-point string map represents the method of undetermined coefficients. The numerator of $q = 1$ can be chosen in the functional polynomial form of degree 2 with coefficients $\beta_0, \ldots, \beta_5$ as follows:

$$\begin{aligned} P_{q=1,{\rm Num}}^{(2)}(\tau, h) \;&=\; \beta_0 p^2(\tau+h) + \beta_1 p^2(\tau) + \beta_2 p^2(\tau+l_{\rm s}) \\ &+\; \beta_3 p(\tau)p(\tau+h) + \beta_4 p(\tau)p(\tau+l_{\rm s}) + \beta_5 p(\tau+h)p(\tau+l_{\rm s})\,. \end{aligned} \tag{13}$$

Again, the Dirichlet conditions $P^{(2)}_{q=1,\mathrm{Num}}(\tau,0) = P_{q=1,\mathrm{Num}}(\tau,l_{\mathrm{s}}) = 0$ yield $P^{(2)}_{q=1,\mathrm{Num}} = \beta_0(p(\tau)-p(\tau+h))(p(\tau+l_{\mathrm{s}})-p(\tau+h))$ with arbitrary β_0. The overlooked denominator part of fraction $P^{(2)}_{q=1}$ then servers as a normalization factor.

Another interesting issue is the generalizing 1-end-point string to include the effect of many length scales

$$P^{(N_{l_{\mathrm{s}}})}_q(\tau,h;\{l\}) = \prod_{i=1}^{N_{l_{\mathrm{s}}}} f_q\left(\frac{p(\tau+l_i)-p(\tau+h)}{p(\tau+h)}\right), \tag{14}$$

which relies on the sequence $\{l\} \equiv \{l_i,\ i = 1,\ldots,N_{l_{\mathrm{s}}}\}$, including the end points $(\min_{i=1,\ldots,N_{l_{\mathrm{s}}}} l_i$ and $\max_{i=1,\ldots,N_{l_{\mathrm{s}}}} l_i)$ as well as the $N_{l_{\mathrm{s}}}-2$ interior node points that divide the string map into the sequence of unfixed segments of the non-uniform length (in general).

4. Spin as a Profit for Long

Discrete dynamical rules are implemented where the string state is sequentially transferred to the past and stored by means of instant replicas. In this model the m'th string of replica system is described by the tuple

$$\left[\{X^{(m)}_{k,s}(h)\};\ m=0,1,\ldots,M;\ h=0,\ldots,h_{\mathrm{op}};\ S^{(m)}\in\{-1,1\}\right] \tag{15}$$

including string coordinates and additional one spin supplementary variable $S^{(m)}$. The meaning of the spin is the same as in particle physics where there are two possibilities for the spin orientation of particle [22]. Suppose the long position is opened at the quote h_{op} and closed at $h_{\mathrm{cl}} > h_{\mathrm{op}}$, then $S^{(m)}$ describes profit when $S^{(m)} = +1$ or loss when $S^{(m)} = -1$. In the case of buy order the sign of $S^{(M)}$ can be deduced from the price change according $S^{(M)} = \mathrm{sgn}(x_{\mathrm{b}}(h_{\mathrm{cl}}) - x_{\mathrm{a}}(h_{\mathrm{op}}))$.

The differences between string states can be measured by the string-string Hilbert Lp-distance as it follows

$$D^{(m,M)}_p = \left[\frac{1}{d_{\mathrm{X}} h_{\mathrm{op}}} \sum_{h=0}^{h_{\mathrm{op}}} \sum_{j=0}^{d_{\mathrm{X}}} |X^{(M)}_j(h) - X^{(m)}_j(h)|^p\right]^{1/p}, \tag{16}$$

where m, M are string-replica indices. The fuzzy character of the prediction of the spin variable of M-th replica is described by means of

$$\overline{S}^{(M)} = \sum_{m=0}^{M_{\mathrm{red}}} S^{(m)} w^{(m,M)}, \quad M_{\mathrm{red}} = M - (h_{\mathrm{cl}} - h_{\mathrm{op}}), \tag{17}$$

which includes Boltzmann-like weights

$$w^{(m,M)} = \frac{\exp\left(-c_D D^{(m)}_p / \overline{D}^{(M)}_p\right)}{\sum_{m'=0}^{M_{\mathrm{red}}} \exp\left(-c_D\, D^{(m')}_p / \overline{D}^{(M)}_p\right)}, \tag{18}$$

where the inter-replica distance is rescaled by the mean

$$\overline{D}_p^{(M)} = \frac{1}{M_{\rm red}+1} \sum_{m=0}^{M_{\rm red}} D_p^{(m,M)} \,. \tag{19}$$

4.1. Symbolic Dynamics and Inter-string Information Transfer

We postulated dynamics as ordered moves of the data. The moves originates from the initial string $X_j^{(M)}(h)$ including transformation of data. The information then passes sequentialy along copies $X_j^{(m)}$ in the sence of decremented replica index m according to

$$\begin{aligned}
X_j^{(M)}(h) &\leftarrow X_j(h)\,, \quad S^{(M)} \leftarrow \text{sgn}(x_{\rm b}(h_{\rm cl}) - x_{\rm a}(h_{\rm op}))\,,\\
X_j^{(M-1)}(h) &\leftarrow X_j^{(M)}(h)\,, \quad S^{(M-1)} \leftarrow S^{(M)}\,,\\
&\ldots\\
&\ldots\\
X_j^{(1)}(h) &\leftarrow X_j^{(2)}(h), \qquad S^{(1)} \leftarrow S^{(2)},\\
X_j^{(0)}(h) &\leftarrow X_j^{(1)}(h)\,, \qquad S^{(0)} \leftarrow S^{(1)}\,.
\end{aligned} \tag{20}$$

We see that information becomes lost at $X_j^{(m=0)}$. This metod could be useful for trading algorythm especially for selection of final trades.

5. Symmetry with Respect to $p(.) \to 1/p(.)$ Transform

The currency pairs can be separated into *direct* and *indirect* type. In a direct quote the *domestic* currency is the base currency, while the *foreign* currency is the quote currency. An *indirect* quote is just the opposite. Therefore, it would be interesting to take this symmetry into account. Hence, one can say that this two-fold division of the market network admits *duality symmetry*. Duality symmetries are some of the most interesting symmetries in physics. The term *duality* is used to refer to the relationship between two systems that have different descriptions but identical physics (identical trading operations).

Let us analyze the 1-end-point elementary string map when the currency changes from direct to indirect. The change can be formalized by means of the transformation

$$\hat{\mathcal{T}}_{\rm id} \,:\, P\{p(.)\} \to \overline{P}\{p(.)\} \equiv P\{1/p(.)\}\,, \tag{21}$$

For the 1-end-point map model of the string, Eq.(5), we obtained

$$\hat{\mathcal{T}}_{\rm id} P_q^{(1)}(\tau,h) = \overline{P}_q^{(1)}(\tau,h) = f_q\left(\frac{p(\tau)-p(\tau+h)}{p(\tau)}\right)\,. \tag{22}$$

Let us consider two-member space of maps $V_P^{(1)} = \{P_q^{(1)}, \overline{P}_q^{(1)}\}$. Important, we see that $\hat{\mathcal{T}}_{\rm id}$ preserves the Dirichlet boundary conditions, in addition, the identity operator $\hat{\mathcal{T}}_{\rm id}^2$ leaves the elements of $V_P^{(1)}$ unchanged. The space $V_P^{(1)}$ is closed under the left action of $\hat{\mathcal{T}}_{\rm id}$. These ideas are straightforward transferable to the 2-end-point string points.

Now we omit the notation details and proceed according to Eq.(21). The map $P(.)$ is decomposable into a sum of symmetric and antisymmetric parts

$$P^{\rm S} = \frac{1}{2}(P + \overline{P})\,, \qquad P^{\rm A} = \frac{1}{2}(P - \overline{P}), \tag{23}$$

respectively. Due to of normalization by $1/2$, we get the projection properties

$$\hat{\mathcal{T}}_{\rm id} P^{\rm S} = P^{\rm S}\,, \qquad \hat{\mathcal{T}}_{\rm id} P^{\rm A} = -P^{\rm A}\,. \tag{24}$$

To be more concrete, we choose $q = 1$ and obtain

$$P^{(1),\rm S}_{q=1} = 1 - \frac{1}{2}\left[\frac{p(\tau)}{p(\tau+h)} + \frac{p(\tau+h)}{p(\tau)}\right]\,, \qquad P^{(1),\rm A}_{q=1} = \frac{1}{2}\left[\frac{p(\tau)}{p(\tau+h)} - \frac{p(\tau+h)}{p(\tau)}\right]\,. \tag{25}$$

and

$$P^{(2),\rm A}_{1} = \frac{1}{2}\left[\frac{p(\tau)}{p(\tau+l_{\rm s})} - \frac{p(\tau+l_{\rm s})}{p(\tau)} + \frac{p(\tau+h)}{p(\tau)} - \frac{p(\tau)}{p(\tau+h)} + \frac{p(\tau+l_{\rm s})}{p(\tau+h)} - \frac{p(\tau+h)}{p(\tau+l_{\rm s})}\right], \tag{26}$$

$$P^{(2),\rm S}_{1} = 1 + \frac{1}{2}\left[\frac{p(\tau+l_{\rm s})}{p(\tau)} + \frac{p(\tau)}{p(\tau+l_{\rm s})} - \frac{p(\tau)}{p(\tau+h)} - \frac{p(\tau+h)}{p(\tau)} - \frac{p(\tau+h)}{p(\tau+l_{\rm s})} - \frac{p(\tau+l_{\rm s})}{p(\tau+h)}\right]\,.$$

We see that the $P^{(1),\rm S}_{q=1}$ and $P^{(2),\rm S}_{q=1}$ maps acquire formal signs of the systems with $T-$*dual symmetry* [2]. When the world described by the closed string of the radius R is indistinguishable from the world of the radius $\propto 1/R$ for any R, the symmetry manifests itself by $(R \pm \text{const.}/R)$ terms of the mass squared operator. The correspondence with our model becomes apparent one assumes that R corresponds to the ratio $p(\tau)/p(\tau+h)$ in Eq.(25). However, we must also refer a reader to an apparently serious difference that in our model we do not consider for the moment the compact dimension. One can also find in the option price dynamics some real example of duality symmetry [23]. Concretely put-call duality which means "A call to buy foreign with domestic is equal to a put to sell domestic for foreign." Also most questions will not spell out what is domestic or foreign but let you decide what is the underlying asset and which is the strike asset.

5.1. $\mathcal{T}_{\rm id}$ Transform under the Conditions of Bid-ask Spreads

Simply, the generalization can also be made with allowing for currency variables which appear as a consequence of the transaction costs [24]. The occurrence of ask-bid spread complicates the analysis in several ways. Instead of one price for each currency, the task requires the availability to two prices. The impact of ask-bid spread on the time-series properties has been studied within the elementary model [25].

Thus, for the purpose of a thorough and more realistic analysis of the market information, it seems straightforward to introduce generalized transform

$$\hat{\mathcal{T}}^{\rm ab}_{\rm id} P\{\, p_{\rm ask}(.), p_{\rm bid}(.)\,\} = \overline{P}\{\, 1/p_{\rm bid}(.), 1/p_{\rm ask}(.)\,\}\,, \tag{27}$$

which converts to Eq.(22) in the limit of vanishing spread.

6. Mapping to the Model of 2D Brane

Clearly, there is a possibility to go beyond a string model towards more complex maps including alternative spread-adjusted currency returns. This is extension of string theory into the higher dimensions from the string lines into the membranes called D-Branes [26]. Formally, the generalized mapping onto the 2D brane with the $(h_1, h_2) \in < 0, l_s > \times < 0, l_s >$ coordinates which vary along two extra dimensions could be proposed in the following form:

$$\begin{aligned} P_{2D,q}(\tau, h_1, h_2) &= f_q \left(\left(\frac{p_{ask}(\tau + h_1) - p_{ask}(\tau)}{p_{ask}(\tau + h_1)} \right) \left(\frac{p_{ask}(\tau + l_s) - p_{ask}(\tau + h_1)}{p_{ask}(\tau + l_s)} \right) \right. \\ &\times \left. \left(\frac{p_{bid}(\tau) - p_{bid}(\tau + h_2)}{p_{bid}(\tau)} \right) \left(\frac{p_{bid}(\tau + h_2) - p_{bid}(\tau + l_s)}{p_{bid}(\tau + h_2)} \right) \right) . \end{aligned} \tag{28}$$

The map constituted by the combination of "bid" and "ask" quotes is constructed to satisfy the Dirichlet boundary conditions

$$P_{2D,q}(\tau, h_1, 0) = P_{2D,q}(\tau, h_1, l_s) = P_{2D,q}(\tau, 0, h_2) = P_{2D,q}(\tau, l_s, h_2) . \tag{29}$$

In addition, the above construction, Eq.(28), has been chosen as an explicit example, where the action of $\hat{\mathcal{T}}_{id}^{ab}$ becomes equivalent to the permutation of coordinates

$$\hat{\mathcal{T}}_{id}^{ab} P_{2D,q}(\tau, h_1, h_2) = P_{2D,q}(\tau, h_2, h_1) . \tag{30}$$

Thus, the symmetry with respect to interchange of extra dimensions h_1, h_2 can be achieved through $P_{2D,q} + \hat{\mathcal{T}}_{id}^{ab} P_{2D,q}$. In a straightforward analogous manner one can get an antisymmetric combination $P_{2D,q} - \hat{\mathcal{T}}_{id}^{ab} P_{2D,q}$. For a certain instant of time we proposed illustration which is depicted in Fig.(1)(b).

At the end of this subsection, we consider the next even simple example, where mixed boundary conditions take place. Now let the 2-end-point string be allowed to pass to the 1-end-point string by means of the homotopy $P_{q1,q2}^{(1,2)}(\tau, h, \eta) = (1-\eta) P_{q1}^{(1)}(\tau, h) + \eta P_{q2}^{(2)}(\tau, h)$ driven by the parameter η which varies from 0 to 1. In fact, this model can be seen as a variant of the 2D brane with extra dimensions h and η.

6.1. Partial Compactification

In the frame of the string theory, the compactification attempts to ensure compatibility of the universe based on the four observable dimensions with twenty-six dimensions found in the theoretical model systems. From the standpoint of the problems considered here, the compactification may be viewed as an act of the information reduction of the original signal data, which makes the transformed signal periodic. Of course, it is not very favorable to close strings by the complete periodization of real input signals. Partial closure would be more interesting. This uses pre-mapping

$$\tilde{p}(\tau) = \frac{1}{N_m} \sum_{m=0}^{N_m - 1} p(\tau + l_s m) , \tag{31}$$

where the input of any open string (see e.g. Eq.(3), Eq.(7)) is made up partially compact.

Thus, data from the interval $< \tau, \tau + l_{\rm s}(N_{\rm m} - 1) >$ are being pressed to occupy "little space" $h \in < 0, l_{\rm s} >$. We see that as $N_{\rm m}$ increases, the deviations of $\tilde{p}$ from the periodic signal become less pronounced. The idea is illustrated in Fig.(1)(c),(d). We see that the states are losing their original form (a),(b) are starting to create ripples.

For example, one might consider the construction of the $(\tilde{D} + 1)$-brane

$$f_q \left(\frac{p(\tau + h_0) - p(\tau)}{p(\tau + h_0)} \right) \prod_{j=1}^{\tilde{D}} f_q \left(\frac{\tilde{p}_j^{(\pm)}(\tau + h_j) - \tilde{p}_j^{(\pm)}(\tau)}{\tilde{p}_j^{(\pm)}(\tau + h_j)} \right) \tag{32}$$

maintained by combining $(\tilde{D} + 1)$ 1-end-point strings, where partial compactification in $\tilde{D}$ extra dimensions is supposed. Of course, the construction introduces auxiliary variables $\tilde{p}_j^{(\pm)}(\tau) = \sum_{m=0}^{N_{\rm m},j-1} p(\tau \pm m\, l_{{\rm s},j})$.

7. Statistical Investigation of 2-end-point Strings

7.1. The Midpoint Information about String

In our present work, the strings and branes represent targets of physics-motivated maps which convert an originally dynamic range of currency data into the static frame. Of course, the data shaped by the string map have to be studied by the statistical methods. However, the question remains open about the selection of the most promising types of maps from the point of view of interpretation of their statistical response.

Many of the preliminary numerical experiments we performed indicating that the 2-end-point strings with a sufficiently high q (in this work we focus on $q = 6$, but other unexplored values may also be of special interest) yield interesting statistical information including focus on rare events. Unfortunately, there is difficult or impossible to be exhaustive in this aspect. Figure(3) shows how $< P_6^{(2)}(\tau, h) >$ and the corresponding dispersion σ_{P_6} change with a string length.

7.2. The Analysis of $P_q(l_{\rm s}/2)$ Distributions

The complex trade fluctuation data can be characterized by their respective statistical moments. In the case of the string map the moments of the ξth order can be naturally considered at the half length

$$\mu_{q,\xi} = \langle\, |P_q^{(N_l)}(\tau, l_{\rm s}/2)|^{\xi/q} \rangle\,. \tag{33}$$

The comparison of the results obtained for the 1-end point and 2-end point strings is depicted in Fig.4. The remarkable difference in the amplitudes is caused by the manner of anchoring. The moments of longer strings are trivially larger.

7.3. Volatility vs. String Amplitude

The volatility as described here refers to the standard deviation of currency returns of a financial instrument within a specific time horizon described by the length $l_{\rm s}/2$. The return volatility at the time scale $l_{\rm s}/2$ is defined by $\sigma_r(l_{\rm s}/2) = \sqrt{r_2(l_{\rm s}/2) - r_1^2(l_{\rm s}/2)}$ using

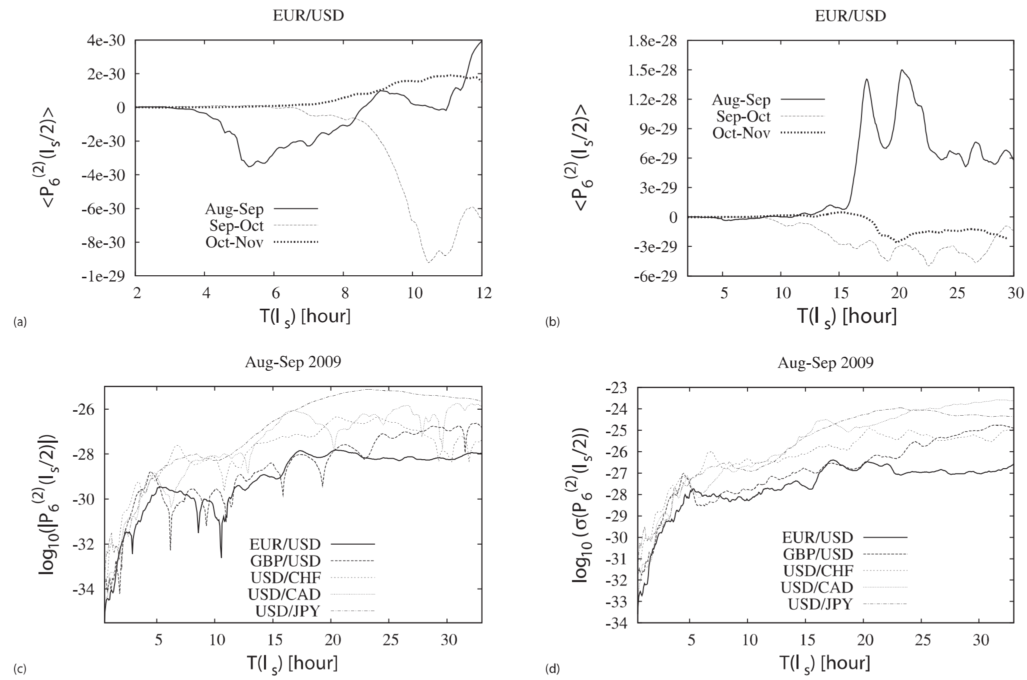

Figure 3. The illustrative calculations carried out for EUR/USD currency. Figure shows the parts (a),(b) which include a view of two different epochs (and their different details). We see the variability of the mean statistical characteristics of the 2-end-point open string. The part (b) turns in sign, but remarkable exceptional scales corresponding to the local maxima and minima remain the same. The string length is expressed in real-time units calculated by means of Eq.(1). In part (c) we present anomalies - peaks roughly common for different currencies. These picture of anomalies are supplemented by dispersions of $P_q^{(2)}(l_s/2)$ (d).

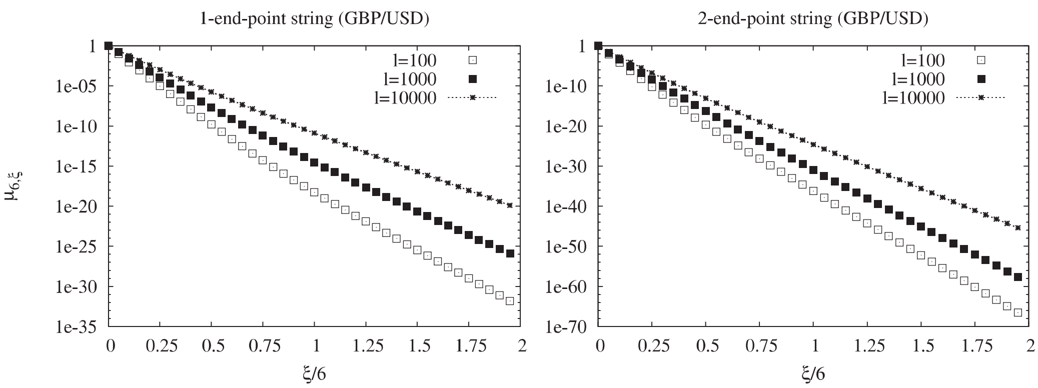

Figure 4. The mid-point fluctuations characterized by the statistical moments defined by Eq.(33). The calculations are carried out for GBP/USD currency rate, for Aug-Sep period, for different kinds of strings for several lengths. We see that fluctuations become more significant as the string size increases. In addition, one may observe the 2-end-point string to be more suppressive to the fluctuations.

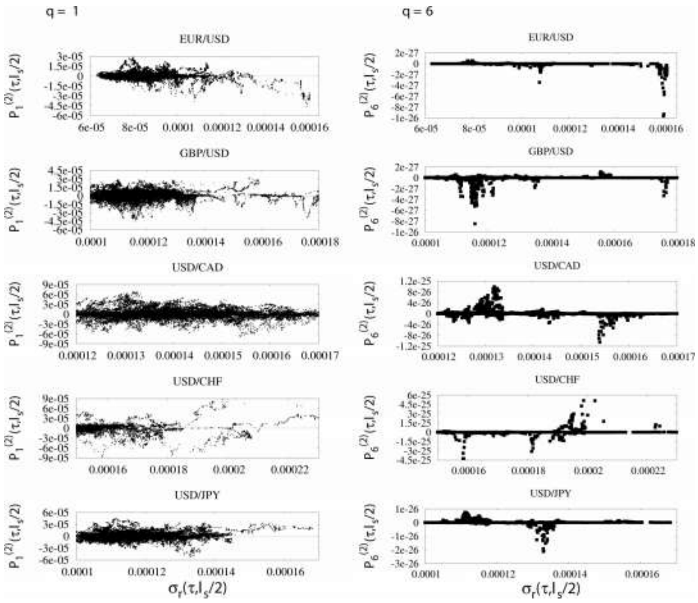

Figure 5. The scatterplot showing the relationship between the volatility $\sigma_r(\tau, l_s/2)$ and the string amplitudes $P_1^{(2)}(l_s/2)$ $(q = 1)$ and $P_6^{(2)}(l_s/2)$ $(q = 6)$, respectively. The separating effect at high q is visible. The plot indicates conservation or brake of the price trend $P_6^{(2)}(l_s/2)$ over the tick time $< \tau, \tau + l_s >$. We see that the trend becomes coupled with the occurrence of specific isolated values of the volatility calculated for $l_s = 10000$; period Aug-Sep.

$r_m(l_s) = \sum_{h=1}^{l_s/2} [(p(\tau + h) - p(\tau + h - 1))/p(\tau + h)]^m$ for $m = 1, 2$. In Fig.(5), the *rate of return volatility* computed at the scale $L = l_s/2$ demonstrates the linkage to the changes in the price trend represented by $P_6^{(2)}(l_s/2)$. Since the trend changes do not follow Gaussian distributions, we have used high q to analyze the impact of rare events. In Fig.(5), we show the identification of the semi-discrete levels of volatility by $q = 6$, while setting $q = 1$ does not uncover common attributes. In the future interest one can compare our return volatility computed from the string amplitude with some volatility estimators or GARCH type of models [27, 28].

8. Learning of Buying and Selling Signals for Currency Pairs

In financial trading, position is a binding commitment to buy or sell a given amount of financial instruments. Open positions remain subject to fluctuations in the exchange rate. Open positions are closed by entering into a trade that takes the opposite position to the original trade. The net effect is to bring the total amount for currency pair back to zero. The bid price ($p_{bid}(\tau)$) is always less than the ask price ($p_{ask}(\tau)$) because brokers pay less than they receive for the same currency pair. The spread represents your cost to trade with broker. The currency pair $p(\tau)$ indicates how much of the quote currency is required to purchase one unit of the base currency; particular currency, which comprises the physical aspects of a nations money supply. For example, EUR/USD = 1.5467 indicates that one euro can buy 1.5467 US dollars.

8.1. Formalism of Trading Signals

Signals are produced by two indicators $I^{(S)}$, $I^{(B)} \in \{0, 1\}$. Signal for opening of sell position is encoded by $I^{(S)} = 1$, whereas $I^{(B)} = 1$ signalizes open for buy

$$I^{(S)}(\tau, \Delta\tau) = 1_{p_{bid}(\tau) > p_{ask}(\tau + \Delta\tau)}, \tag{34}$$

$$I^{(B)}(\tau, \Delta\tau) = 1_{p_{ask}(\tau) < p_{bid}(\tau + \Delta\tau)}. \tag{35}$$

Here τ is the timetick argument; $p_{ask}(\tau + \Delta\tau)$ and $p_{bid}(\tau + \Delta\tau)$ are future values of currency after the time $\Delta\tau$. The symbol 1_{condit} is indicator function taking the value 1 when the condition condit is satisfied (condit = true), 0 when the condition is unsatisfied. In later analysis, we will distinguish symbols $I^{(Y)}(\tau, \tau_M)$ from its prediction $\hat{I}^{(Y)}(\tau, \tau_M)$. The indicator is defined as

$$I^{(Y)}(\tau, \tau_M) = \max\{I^{(Y)}(\tau, 1), I^{(Y)}(\tau, 2), \ldots, I^{(Y)}(\tau, \tau_M)\}, \tag{36}$$

where $Y \in \{S, B\}$; τ_M is the maximum waiting time to open order. The operator max is used for the logical disjunction. It results in 1 whenever one or more of its particular indicators $I^{(Y)}(\tau, \Delta t)$ is equal to 1. This is the process of transformation of data with the goal of highlighting useful information. We call strings as forms of data transformation to analyze sequences of events.

The organization of currency information $p(\tau)$ represents exchange rate

$$p(\tau) = \frac{1}{2}\left(p_{ask}(\tau) + p_{bid}(\tau)\right), \tag{37}$$

or alternatively $p(\tau) = \sqrt{p_{ask}(\tau) p_{bid}(\tau)}$.

8.1.1. String Maps

String map variants of the history influence models is defined as 1-end point string (with end-point $h = 0$)

$$P^{(1)}(\tau, h, Q) = 1 - \left(\frac{p(\tau - h)}{p(\tau)}\right)^Q, \tag{38}$$

$h = 0, 1, 2, \ldots, l_s$, where l_s is the string length.

Process of transferring continuous parameter of deformation Q into discrete counterparts is described

$$Q(j) = Q_{min} + (Q_{max} - Q_{min})\frac{j}{NQ}, \qquad j = 0, 1, \ldots, NQ, \tag{39}$$

where 2-end-point string with end-points ($h = 0$, $h = l_s$) is

$$P^{(2)}(\tau, h, Q) = \left[1 - \left(\frac{p(\tau - h)}{p(\tau)}\right)^Q\right]\left[1 - \left(\frac{p(\tau - l_s)}{p(\tau - h)}\right)^Q\right]. \tag{40}$$

8.2. Decision Making, Binary Classification on the Basis of Nonlinear Interconnected Strings

The architecture single layer forward can be defined as perception (binary classifier) with $2 \times (N_Q + 1) \times (l_s + 1)$ input links and single output $I^{(Y)}$. The activation function is

$$\sigma(x) = \begin{cases} 1 & x > 0 \\ 0 & x \leq 0 \end{cases} . \tag{41}$$

Suggested here prediction model combines the effects of different topology (1-end-point) vs. (2-end-point) strings, within them effects of the rare events controlled by the exponent Q, as well as the effect of tick delay (h)

$$\hat{I}^{(Y)}(\tau, \tau_M) = \sigma \left(\sum_{k=1,2} \sum_{h=0}^{l_s} \sum_{j=0}^{N_Q} W^{(Y)}(k,h,j) P^{(k)}(\tau, h, Q(j)) \right), \tag{42}$$

where $W^{(Y)}(k,h,j)$ interconnections/weights of the group are subjected to the supervised learning technique which minimizes prediction error. One can choose e.q. the parameters $\tau_M = 10$; $N_Q = 12$; $Q_{min} = -6$; $Q_{max} = 6$; $l_s = 50$; $N_m = 10$; and by applying standard learning rules estimate the weights, analyze the relative importance of input units. Moreover examine the stability of the achieved results in the frame of the committee machine class, where several perceptrons are combined into a single response.

9. Correlation Function as Invariant

The meaning of invariant is that something does not change under transformation, such as some equations from one reference frame to another. We want to extend this idea also on the finance market, find some invariants in the finance data and utilize this as the prediction for the following prices. Unfortunately this model is able to define only one step prediction, see the definition below.

We suppose the invariant is in a form of correlation function

$$C_{(t,l_0)} = \sum_{h=l_0}^{h=l} w_h \left(1 - \frac{p_{t-h}}{p_{t-1-h}}\right)\left(1 - \frac{p_{t-1-h}}{p_{t-2-h}}\right), \tag{43}$$

with

$$w_h = \frac{e^{-h/\lambda}}{\sum_{h'=0}^{l} e^{-h'/\lambda}}, \tag{44}$$

including dependence on the time scale parameters l, l_0 and λ. The relative weights satisfy automatically $\sum_{h=0}^{l} w_h = 1$.

A correlation function is a statistical correlation between random variables at two different points in our case the strings in time series. For simplicity as an example we used only one point strings equation (5) with parameter $Q = 1$. Ordinary the correlation function is defined as $C(\tau, l_0) = \langle P^1(\tau, l_0) P^1(\tau + 1, l_0)\rangle$. We suppose the invariant in the form of the correlation function

$$C(\tau, l_0) \quad = \quad \sum_{h=l_0}^{h=l} W(h) \left(1 - \frac{p(\tau - h)}{p(\tau - 1 - h)}\right) \left(1 - \frac{p(\tau - 1 - h)}{p(\tau - 2 - h)}\right), \tag{45}$$

with weight $W(h)$ defined above. We assume the condition of the invariance between close strings in τ and at the next step $\tau + 1$ in time series (It is the exact meaning of the one step prediction) in the form

$$C(\tau, l_0) = C(\tau + 1, l_0). \tag{46}$$

Now we want to find the exact expression for the one step prediction $p(\tau + 1)$. Therefore we evaluate one step correlation invariant equation (46)with initial condition $l_0 = 0$

$$\begin{aligned} W(0) &\quad \left(1 - \frac{p(\tau)}{p(\tau - 1)}\right) \left(1 - \frac{p(\tau - 1)}{p(\tau - 2)}\right) = \\ W(0) &\quad \left(1 - \frac{p(\tau + 1)}{p(\tau)}\right) \left(1 - \frac{p(\tau)}{p(\tau - 1)}\right) + \\ W(1) &\quad \left(1 - \frac{p(\tau)}{p(\tau - 1)}\right) \left(1 - \frac{p(\tau - 1)}{p(\tau - 2)}\right), \end{aligned} \tag{47}$$

which can be rewritten in the more compact form

$$C(\tau, 0) = W(0) \left(1 - \frac{p(\tau + 1)}{p(\tau)}\right) \left(1 - \frac{p(\tau)}{p(\tau - 1)}\right) + C(\tau + 1, 1) \tag{48}$$

and

$$\left(1 - \frac{p(\tau + 1)}{p(\tau)}\right) = \frac{C(\tau, 0) - C(\tau + 1, 1)}{W(0) \left(1 - \frac{p(\tau)}{p(\tau - 1)}\right)}. \tag{49}$$

We finally obtain the prediction

$$p(\tau + 1) = p(\tau) \left(1 + \frac{C(t + 1, 1) - C(t, 0)}{W(0) \left(1 - \frac{p(\tau)}{p(\tau - 1)}\right)}\right), \tag{50}$$

valid for $p(\tau) \neq p(\tau - 1)$. These are general definitions for the one step prediction correlation invariants. In the next section the similar equations can be found also for 2-end-point and 1-end-point mixed string modes with $Q > 0$.

9.1. Prediction Model Based on the String Invariants (PMBSI)

Now we want to take the above-mentioned ideas onto the string maps of finance data. We would like to utilize the power of the nonlinear string maps of finance data and establish some prediction models to predict the behavior of the market similarly as in the works [29, 30, 31]. We suggest the method where one string is continuously deformed into the other.

We analyze 1-end-point and 2-end-point mixed string models. The family of invariants is written using the parametrization

$$
\begin{aligned}
C(\tau,\Lambda) &= (1-\eta_1)(1-\eta_2)\sum_{h=0}^{\Lambda} W(h) \qquad (51)\\
&\times \left(1-\left[\frac{p(\tau)}{p(\tau+h)}\right]^Q\right)\left(1-\left[\frac{p(\tau+h)}{p(\tau+l_s)}\right]^Q\right)\\
&+ \eta_1(1-\eta_2)\sum_{h=0}^{\Lambda} W(h)\left(1-\left[\frac{p(\tau)}{p(\tau+h)}\right]^Q\right)\\
&+ \eta_2\sum_{h=0}^{\Lambda} W(h)\left(1-\left[\frac{p(\tau+h)}{p(\tau+l_s)}\right]^Q\right), \qquad (52)
\end{aligned}
$$

where $\eta_1 \in (-1,1), \eta_2 \in (-1,1)$ are variables (variables which we may be call homotopy parameters), Q is a real valued parameter, and the weight $W(h)$ is chosen in the bimodal single parameter form

$$
W(h) = \begin{cases} 1-W_0\,, & h \le l_s/2\,,\\ W_0\,, & h > l_s/2\,. \end{cases} \qquad (53)
$$

We plan to express $p(\tau+l_s)$ in terms of the auxiliary variables

$$
\begin{aligned}
A_1(\Lambda) &= (1-\eta_1)(1-\eta_2)\sum_{h=0}^{\Lambda} W(h)\left(1-\left[\frac{p(\tau)}{p(\tau+h)}\right]^Q\right), \qquad (54)\\
A_2(\Lambda) &= -(1-\eta_1)(1-\eta_2)\sum_{h=0}^{\Lambda} W(h)\left(1-\left[\frac{p(\tau)}{p(\tau+h)}\right]^Q\right)p^Q(\tau+h)\,, \qquad (55)\\
A_3(\Lambda) &= \eta_1(1-\eta_2)\sum_{h=0}^{\Lambda} W(h)\left(1-\left[\frac{p(\tau)}{p(\tau+h)}\right]^Q\right), \qquad (56)\\
A_4(\Lambda) &= \eta_2\sum_{h=0}^{\Lambda} W(h)\,, \qquad (57)\\
A_5(\Lambda) &= -\eta_2\sum_{h=0}^{\Lambda} W(h)\,p^Q(\tau+h)\,. \qquad (58)
\end{aligned}
$$

Thus the expected prediction form reads

$$
\hat{p}(\tau_0+l_{\mathrm{pr}}) = \left[\frac{A_2(\Lambda)+A_5(\Lambda)}{C(\tau_0-l_{\mathrm{s}},\Lambda)-A_1(\Lambda)-A_3(\Lambda)-A_4(\Lambda)}\right]^{1/Q}, \qquad (59)
$$

where we use the notation $\tau = \tau_0 + l_{\mathrm{pr}} - l_s$. The derivation is based on the invariance

$$
C(\tau, l_s - l_{\mathrm{pr}}) = C(\tau - l_{\mathrm{pr}}, l_s - l_{\mathrm{pr}})\,, \quad \Lambda = l_s - l_{\mathrm{pr}}\,, \qquad (60)
$$

where l_{pr} denotes the prediction scale.

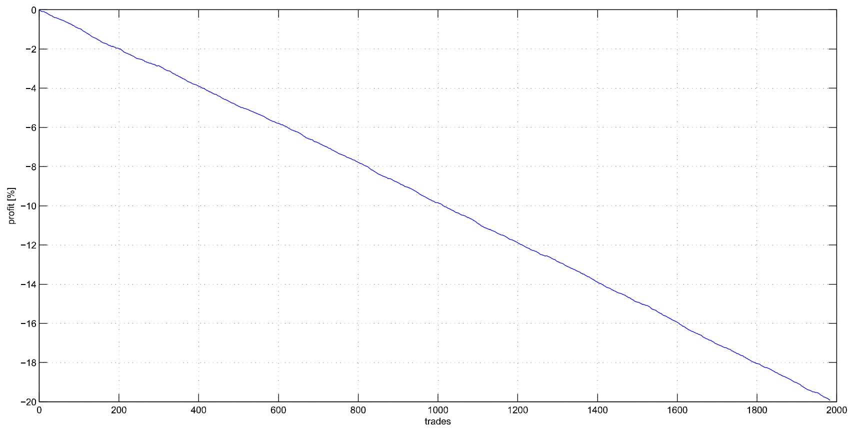

Figure 6. The profit of the model on the EUR/USD currency rate with transaction costs included dependence on trades for one year period.

The model was tested for various sets of parameters l_s, $l_{\rm pr}$, η_1, η_2, Q and the new parameter ϵ which is defined as

$$\epsilon = |C(\tau, l_s - l_{\rm pr}) - C(\tau - l_{\rm pr}, l_s - l_{\rm pr})| \tag{61}$$

and describes the level of invariance in real data. The best prediction (the best means that the model has the best ability to estimate the right price) is obtained by using the following values of parameters

$$l_s = 900, \quad l_{\rm pr} = 1, \quad \eta_1 = 0, \quad \eta_2 = 0, \quad Q = 6, \quad \epsilon = 10^{-10}. \tag{62}$$

The graphical descriptions of prediction behavior of the model with and without transaction costs on the EUR/USD currency rate of the forex market are described in Figs 6-9. During a one year period the model lost around 20% of the initial money. It executed 1983 trades (Fig 6) where only 10 were suggested by the model (and earned money) and the rest of them were random (which can be clearly seen in Figs 8, and 9). The problem of this model is its prediction length (the parameter $l_{\rm pr}$), in this case it is one tick ahead. The price was predicted correctly in 48.57% of all cases (16201 in one year) and from these 48.57% or numerally 7869 cases only 0.13% or numerally 10 were suitable for trading. This small percentage is caused by the fact that the price does not change too often one tick ahead. One could try to raise the prediction length to find more suitable cases for trading. This is only partly successful because the rising parameter $l_{\rm pr}$ induces a loss of the prediction strength of the model. For example when $l_{\rm pr} = 2$ (two ticks ahead) the prediction strength decreases from around 50% to 15%.

The problem is that the invariant equation (46) is fulfilled only on the very short period of the time series due to the very chaotic nature of financial data behavior. Therefore the PMBSI is effective only on the one step prediction where there is very low probability

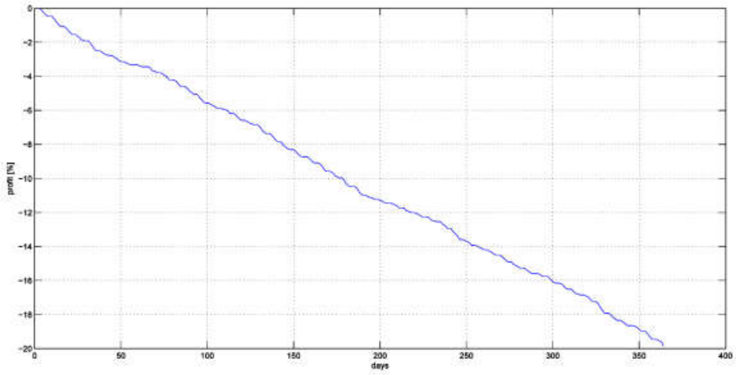

Figure 7. The profit of the model on the EUR/USD currency rate with transaction costs included dependence on days for one year period.

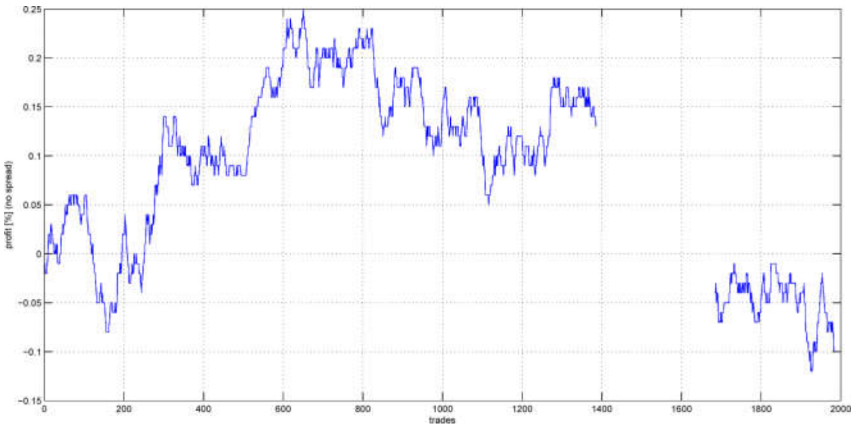

Figure 8. The profit of the model on the EUR/USD currency rate without transaction costs included dependence on trades for one year period.

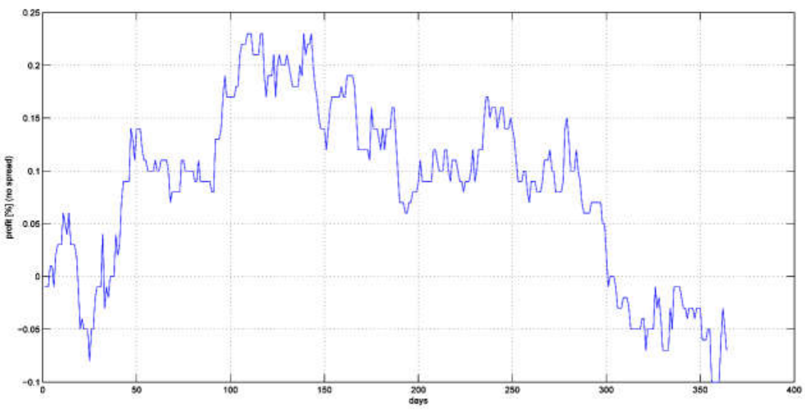

Figure 9. The profit of the model on the EUR/USD currency rate without transaction costs included dependence on days for one year period.

that time series change significantly. The situation, however, is different for more steps prediction where there is, on the contrary, a very high probability of big changes in time series to occur, and the following predictions have rather small efficiency in such cases. The only way how to establish better prediction also for more steps prediction is to choose the right weights equation (44). The right and optimized weights should considerably extend the interval where equation (46) is fulfilled. Therefore it is also our task in the future work.

9.2. Experimental Setup

The experiments were performed on two time series. The first series represented artificial data namely a single period of a sinusoid sampled by 51 regularly spaced samples. The second time series represented proprietary financial data sampled daily over a period of 1295 days. The performance of PMBSI was compared to SVM and to naive forecast. There were two error measures used, mean absolute error (MAE) and symmetric mean absolute percentage error (SMAPE) defined as follows:

$$MAE = \frac{1}{n}\sum_{t=1}^{n} |A_t - F_t| \,, \quad (63)$$

$$SMAPE = \frac{100}{n}\sum_{t=1}^{n} \frac{|A_t - F_t|}{0.5(|A_t| + |F_t|)} \,, \quad (64)$$

where n is the number of samples, A_t is the actual value and F_t is the forecast value. Each time series was divided into three subsets: training, evaluation and validation data. The time ordering of the data was maintained; the least recent data were used for training, while the more recent data were used to evaluate the performance of the particular model with the given parameters' setting. The best performing model on the evaluation set (in terms of MAE) was chosen and made to forecast for the validation data (the most recent) that were never used in the model optimization process. Experimental results on the evaluation and validation data are presented below. The parameters of the models were optimized by trying all combinations of parameters sampled from given ranges with a sufficient sampling rate. Naturally, this process is slow but it enabled us to get an image of the shape of the error surface corresponding to the given settings of parameters and ensured that local minima are explored. The above approach was used for both, PMBSI and SVM. The SVM models were constructed so that the present value and a certain number of the consecutive past values comprised the input to the model. The input vector corresponds to what will be referred to here as the *time window* with the length l_{tw} (representing the equivalent of the length of the string map l_s by PMBSI).

10. Comparison

There was a preliminary experimental analysis performed of the PMBSI method performed. The goal was to evaluate the prediction accuracy, generalization performance, convenience of the method in terms of the operator effort needed to prepare a working model, computational time and other aspects of the PMBSI method that may have become obvious during the practical deployment. SVM was chosen as a benchmark. The experimental data comprised two sets: artificial data (a single period of a sinusoid) and real world data (financial, price development). We will provide a brief conclusion of the analysis here. Each time series was divided into three subsets for training, testing and validation. The results were calculated on the validation sets that have been entirely absent in the process of optimization of parameters.

The PMBSI predictor does not undergo a training process that is typical for ANN and SVM where a number of free parameters must be set (synaptic weights by ANN, α coefficients by SVM). PMBSI features a similar set of weights (W) but often very small and calculated analytically. The parameters to be optimized are only four: ls, Q, η_1, η_2. This, clearly, is an advantage. On the other hand the optimal setting of the parameters is not easy to find as there are many local minima on the error surface. In this analysis the optimal setting was found by testing of all combinations of parameters from given ranges. Fig. 10 shows the Mean Absolute Error (MAE) of the 5-steps ahead forecast of the financial time series corresponding to various settings of ls and Q ($\eta_1, \eta_2 = 0$). But the figure makes it also obvious that PMBSI's performance is approximately the same for a wide range of settings on this data.

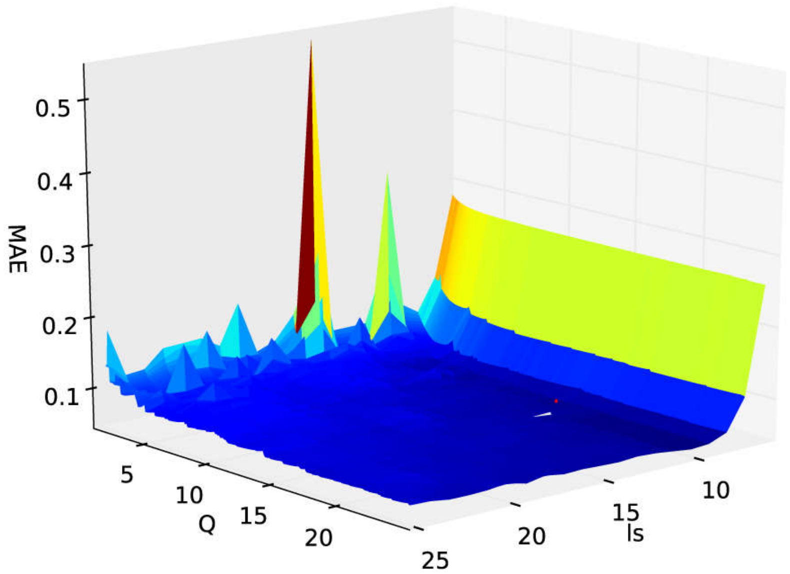

Figure 10. MAE corresponding to various settings of ls and Q on the financial data. The red dot is the global minimum of MAE.

For PMBSI to work the elements of time series must be non-zero otherwise the method will return *not a number* forecasts only. The input time series must then be modified by adding a constant and the forecast by subtracting the same constant. Even so the algorithm returned a *not a number* forecast in approx. 20% of the cases on the financial data. In such cases the last valid forecast was used. Due to reasons that are presently being evaluated the

Table 1. Experimental results on artificial time series

Method	l_{pr}	MAE eval	MAE valid	SMAPE valid
PMBSI	1	0.000973	**0.002968**	**8.838798**
	2	0.006947	0.034032	14.745538
	3	0.015995	0.161837	54.303315
Iterated PMBSI	1	-	-	-
	2	0.003436	0.011583	10.879313
	3	0.008015	0.028096	14.047025
SVM	1	0.011831	0.007723	10.060302
	2	0.012350	**0.007703**	**10.711573**
	3	0.012412	**0.007322**	**11.551324**
Naive forecast	1	-	0.077947	25.345352
	2	-	0.147725	34.918149
	3	-	0.207250	41.972591

Table 2. Optimal PMBSI parameters

l_{pr}	l_s	Q	η_1	η_2
1	2	0.30	0.80	-0.20
2	5	0.10	0.80	-0.60
3	8	0.10	0.80	-0.60

accuracy of PMBSI is matching and even outperforming SVM for a single step predictions but rapidly deteriorates for predictions of more steps ahead. Iterated prediction of several steps ahead using the single step PMBSI predictor improves the accuracy significantly. The sinusoid used for experiments was sampled by 51 points, the positive part of the wave was used for optimization of the parameters and the rest for validation (approx. 50-50 division). Fig. 11 shows the comparison of iterated versus the direct prediction using PMBSI. Table 1 shows the experimental results. The results of the best performing models are highlighted. The optimal l_{tw} for SVM was 3 for all predictions. Table 2 shows the optimal settings found for PMBSI. For $l_{pr} = 1$ when PMBSI outperformed linear SVM the optimal length of the string map was shorter than the optimal time window for SVM; in the remaining cases it was significantly longer.

11. Prediction Model Based on the Deviations from the Closed String/Pattern Form (PMBCS)

For the next trading strategy we want to define some real values of the string sequences. Therefore we define the momentum which acquired values from the interval $(0, 1)$. The

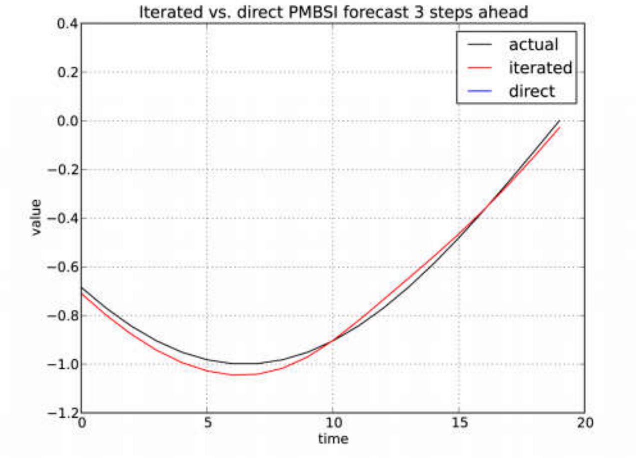

Figure 11. Iterated and direct prediction using PMBSI on artificial data.

momentum M is not strictly invariant as in the previous model of the time series in its basic definition. It is a trading strategy to find such a place in the forex time series market where M is exactly invariant or almost invariant and we can predict increasing or decreasing of prices with higher efficiency. For example our predictor somewhere in the time series has 55% of efficiency to predict the movement of price but in the invariant place of our trading strategy where Eqs. (61), and (65) are almost invariant the efficiency of our predictor increased to 80%. Therefore the idea to find the invariant in time series plays a crucial role in our trading strategy but one still needs to find an appropriate expression for such a prediction.

To study the deviations from the benchmark string sequence we define momentum as

$$M_{(l_s,m;Q,\varphi)} = \left(\frac{1}{l_s+1} \sum_{h=0}^{l_s} \left| \frac{p(\tau+h) - p_{\min}(\tau)}{p_{\max}(\tau) - p_{\min}(\tau)} - \frac{1}{2}\left(1 + \cos\left[\frac{2\pi m h}{l_s+1} + \varphi\right]\right) \right|^Q \right)^{1/Q} \quad (65)$$

where

$$p_{\text{stand}}(\tau;h;l_s) \quad = \quad \frac{p(\tau+h) - p_{\min}(\tau;l_s)}{p_{\max}(\tau;l_s) - p_{\min}(\tau;l_s)}, \qquad p_{\text{stand}} \in (0,1),$$

and

$$p_{\max}(\tau;h;l_s) = \max_{h\in\{0,1,2,\ldots,l_s\}} p(\tau+h), \qquad p_{\min}(\tau;h;l_s) = \min_{h\in\{0,1,2,\ldots,l_s\}} p(\tau+h),$$

and φ is a phase of periodic function. The momentum defined above takes the values from the interval $M_{(l_s,m;Q,\varphi)} \in (0,1)$. The periodic function $\cos(\tilde{\varphi})$ in the definition of equation (65) could be substituted by other types of mathematical functions. The results with different kinds of functions could be different.

11.1. Elementary Trading Strategy Based on the Probability Density Function of M

The purpose is to take advantage of it whenever the market conditions are favorable. As in the previous model we are detrending forex data into the one dimensional topological object ”strings” with different parameters. The trading strategy is based on the description of rate curve intervals by one value called the moment of the string. These moments are statistically processed and some interesting values of moments are found. The values directly affect the opening and closing of trade positions. The algorithm works in two complementary phases. The first phase consists of looking for "good" values of moments followed by second phase which uses results from the first phase and opening/closing of trade positions occur. Simultaneously the first phase is looking for new "good" values of moments.

Risk is moderated by a number of allowed trades that the algorithm can open during a certain period. Also it is moderated by two paramaters which affect the selection of suitable moments for trading. The maximum number of trades is 10 per hour. The algorithm is tested on various periods of historical data. The number and period of simultaneously opened trades are monitored all the time.

The first set of parameters describes the moment (simple scalar function of several variables from the interval (0,1)). The first set consists of these parameters: length of moment string (number of ticks or time period), quotient or exponent of moment, frequency of moment function, and phase shift of moment function. The second set of parameters controls trading strategy and consists of these variables: maximum number of simultaneously opened trades, skewness of moments distribution and Sharpe ratio of closed trades. As soon as the algorithm calculates the value of the moment and finds out that the value is "good", then it immediately carries out an appropriate command.

The risk of the algorithm is governed by the second set of parameters and can vary from zero (low risk but also low or zero number of trades) to the boundary values controlled by the model parameters. These boundary values are unlimited but could be easily affected by the skewness and Sharpe ratio. These parameters can limit loss to certain value with accuracy ± 2 percent but also limit overall profit significantly if low risk is desired.

An arbitrage opportunity is taking advantage of the occurrence of a difference in distribution. Opportunity is measured by *Kullback-Leibler* divergence

$$D_{\mathrm{KL}} = \sum_{j(bins)} \mathrm{pdf}(M^+(j)) \log \left(\frac{\mathrm{pdf}(M^+(j))}{\mathrm{pdf}(M^-(j))} \right) \tag{66}$$

where larger D_{KL} means better opportunities ($D_{\mathrm{KL}} > D_{\mathrm{threshold}}$) e.g. when $D_{KL} > D_{threshold}$ it means the buying of Euro against USD could be more profitable. Statistical significance means the smaller the statistics accumulated into bins pdf$(M^+(j))$, pdf$(M^-(j))$, the higher is the risk (M from the selected range should be widespread). The meaning of pdf in the definition of equation above is the probability density function.

More generally we can construct the series of $(l_s + 1)$ price ticks $[p(\tau), p(\tau+1), \ldots, p(\tau+l_s)]$ which are transformed into a single representative real value $M(\tau + l_s)$. Nearly stationary series of $M(\tau + l_s)$ yield statistics which can be split into: branch where M is linked with future uptrend/ downtrend and branch where M is linked with future profit/ loss taking into account transaction costs. Accumulation of pdf(M^{+-}_{long}) means (profit+ / loss-) or pdf$(M^{+-}_{\mathrm{short}})$ (profit+ / loss-). M^+ in equation (66) describes when equation (65) brings profit and M^- loss.

As in the previous section the model was again tested for various sets of free parameters l_s, h, Q, φ. This model can make "more-tick" predictions (in tests it varies from 100 to 5000 ticks). Therefore it is much more successful than the previous model. It is able to make a final profit of around 160% but this huge profit precedes a fall down of 140% of the initial state. It is important to emphasize that all profits mentioned here and below are achieved by using leverage (borrowing money) from 1 to 10. The reason for leverage is the fact that the model could simultaneously open up to 10 positions (one position means one trade i.e. one pair of buy-sell transactions). If one decides not to use any leverage the final profit decreases 10 times. On the other hand, with using the leverage 1 to 20 the final profit doubles itself. Of course, the use of higher leverages is riskier as dropdowns are also higher. There is, for example, in Fig. 12 a dropdown approx. 6% around 600 trades. With

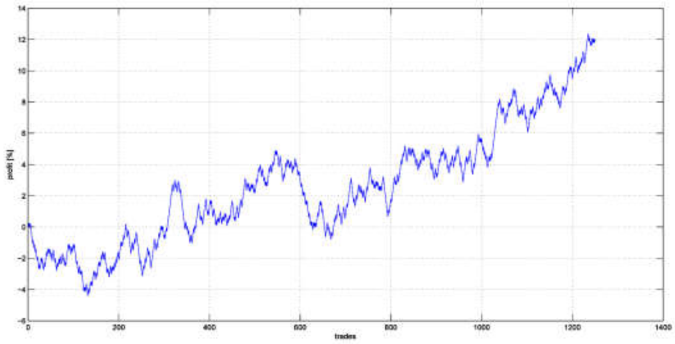

Figure 12. The profit of the model on the EUR/USD currency rate with transaction costs included dependence on trades for one year period.

the use of leverage 1 to 20 this dropdown rises to 12%.

128000 combinations of model's parameters have been calculated. Figures 12-15 describe some interesting cases of the prediction behavior of the model with the transaction cost included on the EUR/USD currency rate of the forex market. Figures 12, and 13 describe the model (one set of parameters) under conditions that the fall down must not be higher than 5%. The best profit achieved in this case is 12%.

In order to sort out the best combinations of parameters it is helpful to use the statistical quantity called the Sharpe ratio. The Sharpe ratio is a measure of the excess return per unit of risk in a trading strategy and is defined as

$$S = \frac{E(R - R_f)}{\sigma}, \tag{67}$$

where R is the asset return, R_f is the return on a benchmark asset (risk free), $E(R-R_f)$ is the mean value of the excess of the asset return over the benchmark return, and σ is the standard deviation of the excess of the asset return. You mention the Sharpe ratio Eq. (67). The values of the Sharpe ratio for the best fit are e.g. for Fig. 15 it is the value 1.896 and for Fig. 16 it is the value 1.953, where as a reference profit we choose a bank with 5% profit.

Figure 14 shows the case where the Sharpe ratio has the highest value from all sets of the calculated parameters. One year profit is around 26% and the maximum loss is slightly over 5%. Figure 15 describes the case requiring a high value of Sharpe ratio and with the aim to gain profit of over 50%.

There exist sufficiently enough cases with high Sharpe ratio which leads to enhancement of the model to create self-education model. This enhancement takes some ticks of data, finds out the best case of parameters (high Sharpe ratio and also high profit) and starts trading with these parameters for some period. Meanwhile, the trading with previously found parameters model is looking for a new best combination of parameters. Figure 16 describes this self-education model where parameters are not chosen and the model itself finds the best one from the financial data and is subsequently looking for the best values for the next trading strategy.

12. Conclusion

We shown that the string theory may motivate the adoption of the nonlinear techniques of the data analysis with a minimum impact of justification parameters. The numerical study recovered interesting fundamental statistical properties of the maps from the data onto string-like objects. The remarkable deviations from the features known under the notion of the efficiently organized market have been observed, namely, for high values of the deformation parameter q.

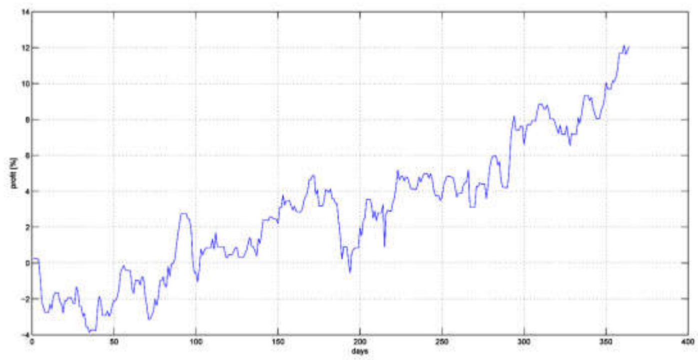

Figure 13. The profit of the model on the EUR/USD currency rate with transaction costs included dependence on days for one year period.

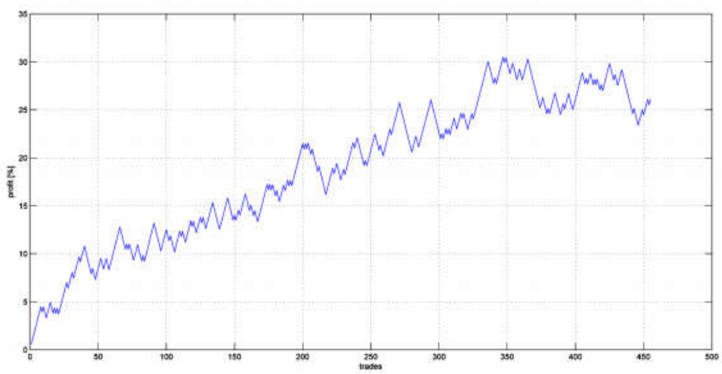

Figure 14. The profit of the model on the EUR/USD currency rate with transaction costs included dependence on trades for one year period.

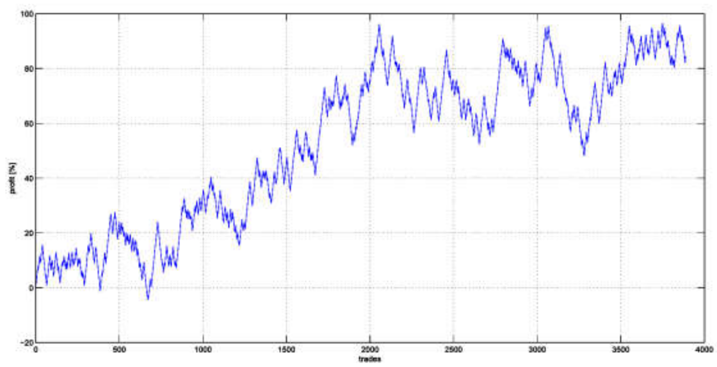

Figure 15. The profit of the model on the EUR/USD currency rate with transaction costs included dependence on trades for one year period.

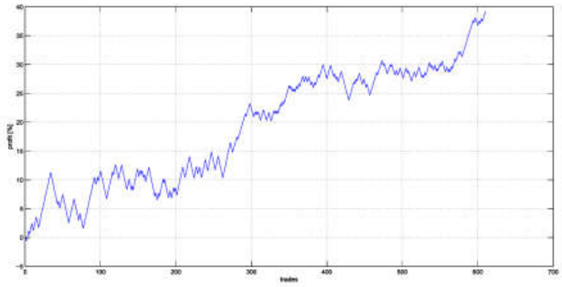

Figure 16. The profit of the self education model on the EUR/USD currency rate with transaction costs included dependence on trades for one year period.

The numerical analysis of the intra-string statistics was supplied qualitatively by the toy models of the maps of the exponential and periodic data inputs. Most of the numerical investigations have been obtained for the open topology; however, we described briefly the ways to partial compactification. The data structures can also be mapped by means of the curled dimension which arises as a sum of periodic data contributions. The idea of the compactified strings can be realized as well by the application of the inverse Fourier transform of the original signal. The interesting and also challenging task represents finding of link between string map and log-periodic behaviour of speculative bubbles of the stock market indices [32, 33]. It would be also interesting to examine R/S analysis of the Hurst exponents [34, 35] for the case of finite strings instead of the usual point prices. The full string dynamics analyzes with different currency on financial market was already published in [36].

The study of string averages exhibited occurrences of the anomalies at the time scales proportional to the string length. We showed that global and common market timescales can be extracted by looking at the changes in the currencies. The extensions of the string models of branes including ask/bid spread were discussed. The membrane 2d-brane approach could be also helpful e.g. for computations of the volatility surface in option pricing [37]. We studied the relationship between the arbitrage opportunities and string statistics. We showed that extraction of the valuable information about the arbitrage opportunities on given currency could be studied by means of the correlation sum which reflected the details of the occupancy of phase-space by differently polarized strings and branes.

We have 5 free parameters in our prediction models. We have also tried out-of-sample tests, however, only using small data samples. We have not encountered ”overfitting” due to the fact that parameters are stable enough within our string theory approach to produce profit even if we slightly change them. For all computations in the second model we are taking bid-offer spreads into account. We are calculating with real values of bid-offer spreads from historical data and it is dependent on where we are simulating on Oanda or Icap etc. A number of trades per day varies from 2 to 15 depending on fit strategy.

We established two different string prediction models to predict the behaviour of forex financial market. The first model PMBSI is based on the correlation function as an invariant and the second one PMBCS is an application based on the deviations from the closed string/pattern form. The financial market invariants could be some other form of definition of scaling laws found in [38] We found the difference between these two approaches. The first model cannot predict the behavior of the forex market with good efficiency in comparison with the second one which, moreover, is able to make relevant profit per year. From the results described we can conclude that the invariant model as one step price prediction is not sufficient for big dynamic changes of the current prices on the finance market. As can be seen in Figs. 8,9 when the transaction costs are switched off the model has some tendency to make a profit or at least preserve fortune. It means that it could also be useful but for other kinds of data, where the dynamics of changes are slower, e.g. for energetic [39] or seismographic data [40] with longer periods of changes. Finally the PBMSI in the form presented in this paper should be applicable with good efficiency only to other kinds of data with smaller chaotic behavior in comparison with financial data.

Moreover PMBSI is a method under development. Unlike SVM or ANN, at this stage PMBSI does not require a training process optimizing a large number of parameters. The experimental results indicate that PMBSI can match or outperform SVM in one step ahead forecasts. Also, it has been shown that finding optimal settings for PMBSI may be difficult but the method's performance does not vary much for a wide range of different settings. Besides the further testing of PMBSI we consider that fast methods for optimization of parameters must be developed. Because of the character of the error surface we have chosen to use evolutionary optimization as the method of choice. After a fast and successful parameters' optimization method is developed optimization of the weighting parameters (Eqs. (44), and (50)) will be included into the evolutionary process.

The profit per year from the second prediction model was obtained from approximately 15 % and more depending on the parameter set from the data we have chosen. This model is established efficiently on the finance market and could be useful to predict future prices for the trading strategy.

Of course the model still needs to be tested further. With the flow of new financial data the model can be more optimized and also, it could become resistant to a crisis. The presented models are universal and could also be used for predictions of other kind of stochastic data. The self-educated models presented in Fig. 16 are very useful because they are able to find on their own the best parameter set from data. These models could also be very helpful for portfolio optimization and financial risk management in the banking sector. Finally we very much hope that the presented approach will be very interesting and useful for a broad spectrum of people working on the financial market.

For another application of string approach, we sketched some hierarchical model of algorithmic chemistry from string atoms to string molecules as a method of adaptive boosting. Discrete dynamical rules are implemented where string state is sequentially transferred to the past and stored by means of instant replicas as was developed in Section 4. We defined a spin of strings which could detect a long-run profit where a fuzzy character of the prediction of the spin variable of N-th replica can be investigated. Finally inter-strings information transfer can be analyzed as an analogy with dynamic of prices or currency at a specified exchange rate options.

13. List of Terms

- String theory: is an active research framework in particle physics where particle are rather 1-dimensional oscillating open or closed lines "strings"
- Brane theory: are membranes of different dimensionality from a one dimensional membrane which is in fact a string lines, including 2, 3 or more dimensional membranes
- Extra dimension: string theory predicts extra dimensions, in classical string theory the number of dimensions is not fixed by any consistency criterion
- Conjugate variable: are pairs of variables mathematically defined in such a way that they become Fourier transform duals of one-another
- T-duality: is a symmetry of quantum field theories with differing classical descriptions,of which the relationship between small and large distances in various string theories is a special case
- Compact dimension: is curled up in itself in very small Planck length and the fact that the dimension is smaller than the smallest particle means that it cannot be observed by conventional means
- Regge slope parameter: was introduced in the quantum theory of string, and its relation to the string tension involves
- Spin in quantum mechanics: is an intrinsic form of angular momentum carried by elementary particles, composite particles (hadrons), and atomic nuclei

• Gâteaux derivative: or directional derivative is often used to formalize the functional derivative commonly used in the calculus of variations and physics

Acknowledgment

The work was supported by the Slovak Academy of Sciences in the framework VEGA Grant No. 2/0037/13. R. Pincak would like to thank the TH division in CERN for hospitality.

References

[1] D. McMahon, ”String theory demystified”, The McGraw-Hill Companies, Inc., (2009).

[2] B. Zwiebach, ”A first course in string theory”, Cambridge university press, (2009).

[3] J. He and M.Deem, PRL 198701, 188 (2010).

[4] W. S. Jung, O. Kwon, F. Wang, T. Kaizoji, H. T. Moon and H. E. Stanley, Physica A 387, 537 (2008).

[5] M. Eryiğit and R. Eryiğit, Physica A 388, 3551 (2009).

[6] P. R. Krishnaiah and L. Kanal, ”Classification, Patterm Recognition, and Reduction of Dimensionality”, North-Holland, Amsterdam (1982).

[7] P. Grassberger and I. Procaccia, Physica D 9, 189 (1983).

[8] Y. Ding, X. Yang, A. J. Kavs and J. Li, Int. J. of Trade, Economics and Finance 1, 320 (2010).

[9] J. Polchinski, ”String Theory”, Cambridge University Press, (1998).

[10] M. B. Green, J. H. Schwarz and E. Witten, ”Superstring theory”,Cambridge University Press, (1987).

[11] Bollerslev, T. (1986), Generalized Autorregressive Conditional Heteroskedasticity, Journal of Econometrics, 31, 307-327.

[12] Engle, R. (1982),Autorregressive Conditional Heteroskedasticity with Estimates of United Kingdom Inflation, Econometrica, 50, 987-1008.

[13] Deistler, M. (1983). The Structure of ARMA Systems in Relation to Estimation. In Geometry and Identification, Proceedings of APSM Workshop on System Geometry, System Identification, and Parameter Estimation, Systems Information and Control, vol. 1, edited by P. E. Caines and R. Hermann, 49-61. Brookline, MS: Math Sci Press.

[14] Box, G.E.P. and G.M. Jenkins (1970) Time series analysis: Forecasting and control,San Francisco: Holden-Day.

[15] Tay, F.E.H. and Cao, L. (2001), Application of support vector machines in financial time-series forecasting. Omega, Vol. 29, pp.309-317.

[16] Kamruzzaman, J. and Sarker, R. (2003), Forecasting of currency exchange rates using ANN: a case study. Proc. IEEE Intl. Conf. on Neur. Net. & Sign. Process. (ICNNSP03), China.

[17] Chen, W-H., Shih, J-Y. and Wu, S. (2006), Comparison of support-vector machines and back propagation neural networks in forecasting the six major Asian stock markets. Int. J. Electronic Finance, Vol. 1, No. 1, pp.49-67.

[18] Vapnik, Vladimir N., The nature of statistical learning theory (1995), Springer-Verlag New York, Inc., isbn: 0-387-94559-8

[19] Bundzel, M.; Sincak, P.; , "Combining Gradient and Evolutionary Approaches to the Artificial Neural Networks Training According to Principles of Support Vector Machines," Neural Networks, 2006. IJCNN '06. International Joint Conference on , pp.2068-2074, doi: 10.1109/IJCNN.2006.246976.

[20] Bundzel, Marek and Kasanický, Tomáš and Frankovič, Baltazár, Building support vector machine alternative using algorithms of computational geometry (2006), Proceedings of the Third international conference on Advances in Neural Networks - Volume Part I, ISNN'06, isbn: 3-540-34439-X, 978-3-540-34439-1, pp. 955–961, Springer-Verlag.

[21] M. C. Mnnix, T. Shimada, R. Schfer, F. L Thomas H. Seligman, T. Guhr and H. E. Stanley, Scientific Reports 2, Article number: 644 doi:10.1038/srep00644 (2012).

[22] W. Greiner, "Relativistic Quantum Mechanics", Springer press, (2000).

[23] J. Fajardo and E. Mordecki, Quantitative Finance 6, 219 (2006).

[24] W. H. Wagner and M. Edwards, Finantial Analytists Journal 49, 65 (1993).

[25] R. Roll, The journal of finance 39, 1127 (1984).

[26] C. V. Johnson, "D-Branes", Cambridge university press, (2003).

[27] B. Bollen, B. Inder, Journal of Empirical Finance 9, 551 (2002).

[28] P. Molnar, International Review of Financial Analysis, In Press, Corrected Proof, Jul 2011 doi:10.1016/j.irfa.2011.06.012.

[29] Jed D. Christiansen, The Journal of Prediction Market 1, 17 (2007).

[30] Ch. Ch. Chang, Ch. Y. Hsieh, Y. Ch. Lin, Applied Economics Letters iFirst, 1 (2011).

[31] J. Wolfers, E. Zitzewitz, Journal of Economic Perspectives 18, 107 (2004).

[32] W. X. Zhou and D. Sornette, Physica A 330, 543 (2003).

[33] W. X. Zhou and D. Sornette, Physica A 337, 243 (2004).

[34] B. Mandelbrot, Review of Economics and Statistics 53, 225 (1971).

[35] M. A. S. Granero, J. E. T. Segovia and J. G. Pérez, Physica A 387, 5543 (2008).

[36] D. Horváth and R. Pincak, Physica A 391, 5172 (2012).

[37] M. J. Kim, S. Y. Lee, D. I. Hwang, S. Y. Kim, I. K. Ko, Physica A 389, 14 (2762).

[38] J.B. Glattfelder, A. Dupuis and R. B. Olsen, Quant. Financ. 11(4), 599 (2011).

[39] A. Lazzarettoa, A. Toffolo, Applied Thermal Engineering 28, 2405 (2008).

[40] R. Stefansson, M. Bonafede, and G. B. Gudmundsson, Bulletin of the Seismological Society of America, 101(4), 1590 (2011).